HHS Public Access

Author manuscript

Clin Cancer Res. Author manuscript; available in PMC 2016 November 01.

Published in final edited form as:

Clin Cancer Res. 2015 November 1; 21(21): 4868–4880. doi:10.1158/1078-0432.CCR-14-1797.

Secreted frizzled related protein 3 (SFRP3) is required for tumorigenesis of PAX3-FOXO1-positive alveolar rhabdomyosarcoma

Julie J.G. Kephart[1], **Rosanne G.J. Tiller**[5], **Lisa E.S. Crose**[2], **Katherine K. Slemmons**[1], **Po-Han Chen**[3], **Ashley R. Hinson**[2], **Rex C. Bentley**[4,5], **Jen-Tsan Ashley Chi**[3,5], and **Corinne M. Linardic**[1,2,5]

[1]Department of Pharmacology and Cancer Biology, Duke University Medical Center, Durham, North Carolina

[2]Department of Pediatrics, Duke University Medical Center, Durham, North Carolina

[3]Department of Molecular Genetics and Microbiology, Duke University Medical Center, Durham, North Carolina

[4]Department of Pathology, Duke University Medical Center, Durham, North Carolina

[5]School of Medicine, Duke University Medical Center, Durham, North Carolina

Abstract

Purpose—Rhabdomyosarcoma is a soft tissue sarcoma associated with the skeletal muscle lineage. Of the two predominant subtypes, known as embryonal (eRMS) and alveolar (aRMS), aRMS has the poorer prognosis, with a 5-year survival rate of <50%. The majority of aRMS tumors express the fusion protein PAX3-FOXO1. As PAX3-FOXO1 has proven chemically intractable, the current study aims to identify targetable proteins that are downstream from or cooperate with PAX3-FOXO1 to support tumorigenesis.

Experimental Design—Microarray analysis of the transcriptomes of human skeletal muscle myoblasts expressing PAX3-FOXO1 revealed alteration of several Wnt pathway gene members, including secreted frizzled related protein 3 (SFRP3), a secreted Wnt pathway inhibitor. Loss-of-function using shRNAs against SFRP3 were used to interrogate the role of SFRP3 in human aRMS cell lines *in vitro* and conditional murine xenograft systems *in vivo*. The combination of SFRP3 genetic suppression and the chemotherapeutic agent vincristine was also examined.

Results—*In vitro*, suppression of SFRP3 inhibited aRMS cell growth, reduced proliferation accompanied by a G_1 arrest and induction of p21, and induced apoptosis. *In vivo*, doxycycline-inducible suppression of SFRP3 reduced aRMS tumor growth and weight by more than three-fold, in addition to increasing myogenic differentiation and β-catenin signaling. The combination of

Corresponding author: Corinne M. Linardic, phone 919-684-3401 (office) / 919-681-3508 (lab); fax 919-681-6906.

Conflict of interest: The authors declare no conflict of interest.

Reprint requests: Send reprint requests to Corinne M. Linardic, Box 102382 DUMC, Durham, NC, 27710; corinne.linardic@dm.duke.edu.

SFRP3 suppression and vincristine was more effective at reducing aRMS cell growth *in vitro* than either treatment alone, and ablated tumorigenesis *in vivo*.

Conclusions—SFRP3 is necessary for the growth of human aRMS cells both *in vitro* and *in vivo* and is a promising new target for investigation in aRMS.

Keywords

SFRP3; PAX3-FOXO1; Rhabdomyosarcoma; Wnt

Introduction

Rhabdomyosarcoma (RMS) is the most common soft tissue sarcoma of childhood and adolescence (1). Thought to be of skeletal muscle in origin, RMS tumors expresses myogenic markers but are unable to form myotubes or functional muscle units, suggesting a defect in differentiation (2, 3). Like other sarcomas, RMS is biologically diverse and presents as a variety of histologies, the most common being embryonal (eRMS; ∼60% of all cases) and alveolar (aRMS; ∼20% of all cases). Therapy for RMS is multi-modal and includes chemotherapy, surgery, and radiation (2). While eRMS 5-year survival rates have improved over the last 30 years, aRMS 5-year survival rates have remained stagnant at less than 50% (4). Understanding the unique molecular abnormalities for each subtype will be critical for designing new therapies. In the case of aRMS, understanding the tumorigenic influence of the associated signature *PAX3-FOXO1* fusion gene will be paramount (5, 6).

The Wnt pathway is an evolutionarily conserved signaling network important for tissue development and homeostasis, directing cell proliferation, polarity, and fate (7) through non-canonical and canonical Wnt/β-catenin branches (8). Canonical Wnt signaling is active when extracellular Wnt binds to a Frizzled (Fzd) receptor, recruiting Dishevelled (DVL) and inhibiting the Axin complex that ordinarily phosphorylates β-catenin (shown in Fig. 1D). Once no longer phosphorylated by glycogen synthase kinase 3 (GSK3) and casein kinase (CK1), β-catenin accumulates in the cytoplasm then translocates to the nucleus where it complexes with T cell factor/lymphoid enhancer factor (TCF/LEF) and activates Wnt target gene transcription (7).

Canonical Wnt signaling is inhibited in the absence of Wnt or in the presence of secreted Wnt pathway inhibitors. This permits β-catenin phosphorylation by CK1 and GSK3 and subsequent degradation by the proteasome. Secreted Wnt inhibitors include the dickkopf-related proteins (DKKs) and the secreted frizzled-related proteins (SFRPs). The SFRPs constitute the largest family of Wnt pathway inhibitors (9, 10), and are divided into two subgroups, with SFRP1, SFRP2, and SFRP5 forming one subgroup, and SFRP3 (also known as FRZB) and SFRP4 forming a second subgroup (9). Since SFRPs share homology to the Fzd receptor, they were first identified as Wnt antagonists that bind and inhibit Wnt in the extracellular space (9). SFRPs may also exert their effects by interacting with each other and Fzd receptors (9).

The Wnt pathway plays a critical role in skeletal myogenesis (11, 12). In myoblasts arising from satellite cells, it promotes myogenic commitment and lineage progression (3, 11). Wnt

signaling also plays an important role in the regeneration of CD45+ stem cells in muscle, promoting hematopoietic (non-myogenic) CD45+ cells to enter a myogenic lineage. Thus Wnt upregulation is critical for myogenic commitment and lineage progression towards fully differentiated muscle. When SFRP3 is added to regenerating muscle *in vitro*, the total number of myotubes formed is decreased (11). Exogenous SFRP3 also reduces the number of CD45+ cells recruited to the myogenic lineage, and the number of mononuclear desmin-expressing myoblasts in regenerating muscle (12). Thus in normal skeletal muscle, SFRP3 exerts an inhibitory effect on myogenic differentiation.

Recently, the Wnt developmental pathway has been implicated in the pathogenesis of RMS. In a murine model of eRMS, Wnt signaling was found downregulated, and activation of Wnt signaling promoted differentiation (13). Similarly, activation of Wnt signaling in human eRMS and aRMS cell lines *in vitro* promoted differentiation (13-15). After identifying changes in the Wnt pathway in a microarray comparing the transcriptomes of human skeletal muscle myoblast (HSMM) cells with and without PAX3-FOXO1 expression, SFRP3 was noted to be upregulated in response to PAX3-FOXO1 expression and investigated further. We discovered that SFRP3 is necessary for aRMS cell growth *in vitro* and tumor xenograft growth in *vivo*. This suggests that SFRP3 is a promising target for future development of therapies for aRMS.

Materials and Methods

Microarray

Microarray analysis of PAX3-FOXO1-expressing HSMMs was previously described (16); the associated dataset has been deposited in the Gene Expression Omnibus database (accession GSE40543). Microarray analysis of SFRP3 shRNA-expressing Rh28 cells was performed as previously described (16). The robust multi-array average (RMA)-normalized data were selected by significance analysis of microarrays (SAM) to identify genes that were consistently induced or repressed by both SFRP3 shRNAs. The associated dataset has been deposited in the Gene Expression Omnibus database (accession GSE67999).

Generation of Cell Lines and Constructs

Human RMS cell lines RD (17), Rh28 (18), and Rh30 (19) were gifts from Tim Triche (Children's Hospital of Los Angeles, CA, USA) in 2005 and Rh36 (20), SMS-CTR (21), and Rh3 (22) were gifts from Brett Hall (Columbus Children's Hospital, OH, USA) in 2006 and cultured as previously described (23). Cell line authentication was performed in 2011 using STR analysis (Promega PowePlex 1.2) conducted by the Fragment Analysis Facility at the Johns Hopkins Genetic Resources Core Facility (Baltimore, MD, USA) and in 2014 (Promega Powerplex 18D) conducted by the Duke University DNA analysis facility (Durham, NC, USA). Human skeletal muscle myoblasts (HSMM, Lonza) stably expressing an empty vector or PAX3-FOXO1 were previously described (16). SFRP3 shRNA sequences were obtained from the RNAi consortium (Broad Institute, Cambridge, MA, USA) and annealed oligos ligated into pLKO.1 puro (Addgene 8453), Tet-pLKO-puro (Addgene 21915), and Tet-pLKO-neo (Addgene 21916) plasmids. HA*-SFRP3 was a gift from Ugo Borello (INSERM/Stem Cell and Brain Research Institute, Cedex, France),

subcloned into the pBABE puro retroviral backbone, and stably expressed in Rh28 cells (24). Nucleotide mismatches between the shRNA sequences (two in SFRP3 sh3, three in SFRP3 sh5) and HA*-SFRP3, render it shRNA-resistant. All cell lines expressing an shRNA or cDNA are polyclonal. Using STR analysis, we retrospectively discovered that the Rh3 and Rh28 cell lines derive from the same patient, and therefore should be considered related (25).

RT-PCR and qPCR

Reverse transcription PCR was performed as previously described (23). Quantitative real-time PCR was performed as previously described (16). Primer sets for this work can be found in Supplementary Table 1.

Immunoblotting

Immunoblotting was performed as previously described, except 50μg of lysate was used per sample (26). The following antibodies were used for immunoblotting: anti-p21 (Santa Cruz #sc-6246), anti-HA (Roche #11583816001), anti-cleaved caspase 3 (Cell Signaling #9661), and anti-actin (Sigma #A5441).

MTT, BrdU, and cell cycle analysis assays

The MTT assay, used as a surrogate for measuring cell growth, and BrdU assay, used to measure cell proliferation, were previously described (26). The cell cycle analysis protocol was previously described and cells were analyzed by the Duke University Flow Cytometry core (27).

Mouse xenograft studies

Rh28 cells stably expressing doxycyline-inducible SFRP3 shRNAs (or empty vector) were implanted subcutaneously into the flanks of SCID/*beige* mice. Mice were monitored twice weekly, and upon observing palpable tumors (Fig. 4 and 6) or a 150 mm^3 tumor (Fig. 5), the drinking water was supplemented with 1 mg/ml doxycycline (Sigma-Aldrich) in 5% w/v sucrose or 5%w/v sucrose (control). Tumors were measured using calipers and tumor volume calculated as $[((width*length)/2)^3]/2$. Mice were sacrificed at 23-24 days (Fig. 4), at 14 days (Fig. 5), or upon reaching an IACUC-defined maximum tumor burden or decline in health (Fig. 4, 5, and 6). This duration of therapy (23-24 days) was chosen as some of the control mice were reaching the maximum tumor burden. For Fig. 5, the later initiation and shorter duration of treatment were chosen to allow for the greatest observation of effects due to SFRP3 suppression before the emergence of resistant cell population. Portions of tumors were preserved in RNAlater (Qiagen) for PCR or formalin-fixed for IHC. All animal studies were conducted in accordance with policies set forth by the Duke University IACUC.

Immunohistochemistry

Paraffin-embedded formalin-fixed xenograft tumor samples were sectioned and stained with H&E (Sigma) to assess morphology. Tumor sections were also labeled with Ki67 (Dako #M7240) and TUNEL (Trevigen #4810-30-K) to assess proliferation and apoptosis, respectively. Slides were evaluated by a pathologist (R.C.B.) with experience in the

evaluation of pediatric sarcomas. Ki67 and TUNEL slides were photographed, and positive and negative cells were counted manually with the aid of cell counting software (ImageJ, NIH). Three tumor sections per treatment condition were labeled with β-catenin (1:200, BD Biosciences #610154). β-catenin slides were photographed (Microscope: Leica Microsystems #DMLB, Camera: Leica Microsystems #DFC425, Software: Leica Microsystems #LAS V 3.7), and the staining intensity of individual cells was counted manually with the aid of cell counting software (ImageJ, NIH).

Drug treatments

For *in vitro* work, vincristine sulfate (Sigma) was dissolved in methanol, diluted in growth media, and added to culture media for final concentrations as indicated. For *in vivo* work, mice were treated with vincristine sulfate (1mg/ml, Hospira) or PBS via intraperitoneal injection at a dose of 1mg/kg weekly for 10 weeks.

Statistics

Unless otherwise noted, data is presented as the mean and SE. Statistical analysis was performed using GraphPad Prism (GraphPad). One-way ANOVA, two-way ANOVA, Log-Rank (Mantel-Cox) Test, and unpaired T-test were used as appropriate. P values were considered significant under 0.05.

Results

Secreted Wnt inhibitors, including SFRP3, are upregulated in PAX3-FOXO1-expressing primary human myoblasts and in human aRMS cell lines

Prior work from our laboratory identified a role for the *PAX3-FOXO1* fusion gene in permitting bypass of HSMM cells past the senescence checkpoint (28), thus priming cells for additional genetic changes that generate the aRMS phenotype (23). To identify genes that are downstream from or cooperate with PAX3-FOXO1 in this event, we performed gene expression analysis of HSMM cells ectopically expressing the *PAX3-FOXO1* fusion cDNA as they transited through pre-senescent and post-senescent stages (16). These cell populations were compared to pre-senescent HSMM cells expressing an empty vector. While approximately 1000 genes were found to be upregulated over 3-fold, one of the pathways that emerged from the analysis was the Wnt pathway.

Review of the gene list revealed changes in both Wnt receptors and ligands, including secreted Wnt activators and inhibitors. In total, seven Wnt pathway members were identified: the secreted inhibitors SFRP1, SFRP3, SFPR4, and DKK2; the canonical and non-canonical Wnt WNT5B (29, 30); and two non-canonical members WNT5A and FDZ5 (Fig. 1A). Other genes known to be altered in PAX3-FOXO1-positive aRMS, including CXCR4, FGFR4, MYOD, MEF2A, served as internal controls for the array (Fig. 1A). Expression of the Wnt family genes was verified by RT-PCR of cDNA generated from the original cell set analyzed in the microarray (Fig. 1B). Because these genes were found upregulated in the setting of ectopic expression of PAX3-FOXO1 in HSMM cells, their expression was next evaluated in three human aRMS cell lines (Rh3, Rh28 and Rh30) and compared to a panel of three human eRMS cell lines (RD, Rh36, SMS-CTR). While we

found SFRP1, SFRP3 and SFRP4 to all be upregulated in aRMS cell lines, SFRP3 was most interesting since its pattern of expression in aRMS cell lines mirrored that in the HSMM cells expressing PAX3-FOXO1, and it was preferentially upregulated in aRMS compared to eRMS cells (Fig. 1C).

Genetic suppression of SFRP3 inhibits aRMS cell growth

To probe the role of SFRP3 in aRMS, we used a loss-of-function approach and generated five lentivirally-delivered shRNA sequences against human SFRP3. Upon stable infection into Rh28 and Rh30 cells, two of the shRNAs reproducibly suppressed SFRP3 expression as measured by RT-PCR (Fig. 2A,B). Monitoring of endogenous SFRP3 at the protein level was not feasible since commercially-available antibodies did not detect SFRP3 protein in our system. As measured by MTT assay, stable expression of the shRNAs in both Rh28 and Rh30 aRMS cells inhibited cell population growth (Fig. 2C,D).

To verify that the growth inhibitory actions of the shRNAs were not due to off-target effects, we sought to concurrently rescue the decreased cell growth with a gain-of-function approach using an ectopically expressed SFRP3. To this end, we took advantage of an shRNA-resistant murine SFRP3 construct with an HA (epitope) tag (24). Since SFRP3 is proteolytically cleaved at both the N and C-termini (31), the HA tag is positioned between the CRD and NTR domains and the construct termed HA*-SFRP3 (Fig. 2E). Using immunoblot to the HA epitope, we verified the ability of the cDNA to be expressed (Fig. 2F), then stably co-expressed it in Rh28 cells containing an empty vector or a doxycycline-inducible shRNAs against SFRP3 (inducible system shown in Supplementary Fig. 1). As predicted, the decreased cell growth observed in the cells expressing SFRP3 shRNAs was largely rescued in the presence of HA*-SFRP3 (Fig. 2G). Taken together, these data suggest that SFRP3 has a pro-growth role in human PAX3-FOXO1-positive aRMS cell lines.

Suppression of SFRP3 in aRMS inhibits cell proliferation and causes a G_1 arrest

To investigate the etiology of the decreased cell growth, we first investigated the possibility that SFRP3 suppression was interfering with cell proliferation. We found that in aRMS cells stably expressing SFRP3 shRNAs, BrdU incorporation declined (Fig. 3A,B), suggesting that loss of function of SFRP3 did indeed inhibit cell proliferation. Since a decrease in cell proliferation can reflect unrecognized differentiation, senescence, or cell cycle arrest, all three processes were further investigated. No consistent or robust differences in the number of differentiated (as assessed by ability to form myotubes and express the myogenic marker MF20) or senescent cells were observed in response to the stable expression of SFRP3 shRNAs in Rh28 cells (data not shown). Similarly, we saw no evidence of Wnt pathway activation (which is required for terminal myogenic differentiation) in aRMS cells stably expressing SFRP3 shRNAs, although in response to Wnt3a-conditioned media and LiCl (a GSK3β inhibitor) they retain the ability to activate β-catenin signaling, similarly to seen previously (15). However, in Rh28 cells both shRNAs caused a 16-22% increase in the percentage of cells accumulated in the G_1 phase of the cell cycle (Fig. 3C). In Rh30 cells, the effect of the shRNAs was more modest, with a 3-5% increase in the percentage of cells at G_1 (Fig. 3D). To investigate mechanism, levels of the cell cycle inhibitor p21 (32) were measured by semi-quantitative RT-PCR and immunoblot. We found p21 upregulated at both

the mRNA (Fig. 3E) and protein (Fig. 3F) levels. Together, these data suggest that inhibition of SFRP3 in aRMS cells inhibits cell proliferation via a G_1 cell-cycle arrest that is partially mediated through p21.

Suppression of SFRP3 in aRMS cells also induces apoptosis

The decrease in cell proliferation observed in aRMS cells expressing SFRP3 shRNAs was much less than the profound decrease observed in overall cell growth. This suggested that another mechanism such as cell death might be contributing. While the previous cell cycle analysis (Fig. 3C,D) showed no change in the sub-G_1 peak (reflective of apoptosis), that analysis had only included adherent cells. And, since cells with SFRP3 shRNAs morphologically demonstrated an increase in the number of floating (non-adherent) cells, to capture possible missed sub-G_1 signal, we next assayed the entire (adherent and non-adherent) cell population by flow cytometry. Rh28 cells expressing SFRP3 shRNAs showed a large increase in the percentage of cells in sub-G_1 (Fig. 3G), while Rh30 cells again showed a more modest increase (Fig. 3H). For confirmation of an apoptotic effect of SFRP3 suppression, we measured cleaved caspase-3 by immunoblot. While no increase in apoptosis as measured by cleaved caspase-3 was observed in the adherent cell population, a significant increase in apoptosis was observed in non-adherent Rh28 cells expressing both SFRP3 shRNAs (Fig. 3I). SFRP3 suppression also increased cleaved caspase 3 in Rh30 cells (Supplementary Fig. 2). In summary, suppression of SFRP3 causes decreased cell proliferation, a cell cycle arrest at G_1, increased p21 expression, and an increase in apoptosis, suggesting that a combination of these mechanisms is responsible for the observed decreased aRMS cell growth.

Suppression of SFRP3 inhibits aRMS tumorigenesis *in vivo*

We next assessed the role of SFRP3 in supporting tumorigenesis *in vivo*, using a conditional subcutaneous xenograft model of aRMS. Since SFRP3 suppression causes aRMS cells to grow poorly, we used a doxycyline-inducible shRNA system to control for effects on tumor implantation. This allowed for expression of the shRNAs after a tumor had formed. SFRP3 sh3 and sh5 were cloned into an inducible vector and tested for their ability to suppress SFRP3 mRNA expression following three days of 4 ug/ml doxycycline (Supplementary Fig. 1A,B). The ability of the inducible shRNA to reduce Rh28 and Rh30 cell growth was also verified (Supplementary Fig. 1C,D).

Xenograft tumors arising from Rh28 cells with a doxycycline-inducible shRNA against SFRP3 or an empty vector were generated, and mice received either control treatment (sucrose water) or doxycycline. Mice receiving the control treatment showed no difference in tumor growth, regardless of SFRP3 shRNA status, showing that in the absence of doxycycline the shRNAs were not leaky (Fig. 4A,C). Mice receiving doxycycline and bearing xenograft tumors from cells expressing empty vector similarly showed robust tumor growth (Fig. 4B,D). However, mice receiving doxycycline and bearing xenografts expressing SFRP3 shRNA3 or shRNA5 showed a profound inhibition of xenograft growth (Fig. 4B,D), with an associated decrease in tumor weight (Fig.4E.) To prove target knockdown, after necropsy levels of human SFRP3 mRNA were measured in the tumors by semi-quantitative RT-PCR and analyzed using densitometry (Fig. 4F). While there was

some variation, tumors in which SFRP3 was suppressed using the shRNAs showed lower levels of SFRP3 than the controls.

To understand the mechanism of decreased tumor growth and identify changes caused by SFRP3 suppression, tumors were embedded, sectioned, and stained for H&E, Ki67, and TUNEL to assess tumor cell morphology, proliferation, and apoptosis, respectively. While H&E showed no obvious changes (data not shown), there was a trend towards a reduction in Ki67 and an increase in apoptosis in tumors bearing SFRP3 shRNAs (Fig. 4G,H), mirroring the observed decrease in proliferation and increase in apoptosis observed *in vitro*.

Suppression of SFRP3 *in vivo* induces markers of differentiation and Wnt pathway activation

While we had not observed a consistent or robust increase in differentiation in RMS cells under conditions of SFRP3 suppression *in vitro*, we nevertheless examined the SQ tumor xenografts for evidence of such, and found that tumors expressing the dox-inducible SFRP3 shRNA constructs under conditions of dox treatment had evidence of myogenic differentiation. Specifically, the early differentiation marker *MyoD* (Fig. 4I) was upregulated in response to SFRP3 sh5, while the intermediate and late markers *Myogenin* (Fig. 4J) and *Myf6* (Fig. 4K) were upregulated in response to both SFRP3 sh3 and sh5. Given the requirement for Wnt signaling during myogenic differentiation, we next examined the same tumors for evidence of Wnt pathway activation using nuclear β-catenin immunohistochemical staining and *Axin2* expression (15, 33-35). While we could not detect an increase in nuclear β-catenin staining in those tumors bearing the SFRP3 shRNAs under conditions of dox treatment (data not shown), we did find *Axin2* modestly upregulated (Fig. 4L).

Since these xenograft tumors were harvested over 20 days after initiation of dox, potentialy permitting tolerance to shRNA expression, we repeated the xenograft experiment but harvested the tumors after only 14 days dox exposure in order to capture early events. As before, those tumors expressing the SFRP3 shRNAs under conditions of dox showed decreased tumor volume and weight (Supplementary Fig. 3A-C), decreased Ki67 (Fig. 5A) and increased TUNEL staining (Fig. 5B). However they also demonstrated an altered morphology (statistically significant fewer cells per field (5C)) and a modest increase in nuclear β-catenin staining (Fig. 5D). Taken together these results suggest that in the *in vivo* setting, suppression of SFRP3 in aRMS does promote myogenic differentiation and Wnt pathway activation.

Given the findings in the xenograft tumors, to gain additional insight into the molecular consequences of SFRP3 suppression we used microarrays to analyze global gene expression after SFRP3 suppression by the two doxycycline-inducible SFRP3 shRNAs (Supplementary Fig. 1A,B) in triplicate. The robust multiarray average (RMA)-normalized data were selected by significance analysis of microarrays (SAM) to identify genes that were consistently induced or repressed by both SFRP3 shRNAs. With the false discovery rate (FDR) of 1.13%, we identified 474 induced and 711 repressed probe-sets (Supplementary Table 2). We analyzed the Gene Ontology (GO) enrichment and found the induced genes were enriched in striated muscle development/differentiation (Supplementary Table 3). In

contrast, the repressed genes were enriched in response to stimulus and cell cycle/mitosis genes (Supplementary Table 3). These results indicate that SFRP3 suppression induced muscle differentiation and repressed proliferation, consistent with the *in vivo* data (Fig. 4G-H, Fig. 5A-D).

Given the role of SFRP3 in Wnt signaling, we also interrogated the microarray data for effects on Wnt-related genes. 109 genes were chosen for analysis (based on the literature and their inclusion in commercially available Wnt-related signaling arrays.) We were most interested in changes seen across both shRNAs, derived by zero-transformation (36), and as expected found downregulation of SFRP3 *(FRZB)* (Fig. 5E, Supplementary Table 4) but also downregulation of Wnt pathway-repressing genes such as *CTBP2* (a transcriptional repressor of TCF, similar to CTBP1 (37)) and NAV2 (which is downstream from APC, (38)). Interestingly, *APC* (which promotes the degradation of β-catenin) was also downregulated by the shRNAs, but just missed the threshold of inclusion. Conversely, we noted upregulation of genes including *CCND1* (cyclin D1) and *SNAI2* (SLUG), both Wnt signaling target genes (39, 40) and *WNT6*, which is known to inhibit myoblast proliferation but induce myoblast elongation (41). Taken together, these results suggest that suppression of SFRP3 in part activates β-catenin/Wnt signaling pathway as we had seen in the tumor xenografts.

SFRP3 suppression in combination with vincristine abrogates aRMS tumorigenesis

Finally, as a pre-clinical assessment of SFRP3 suppression in aRMS, we investigated the role of genetic SFRP3 suppression in combination with chemotherapy, as combination therapy approaches have been successful in treating pediatric malignancies. We hypothesized that combining SFRP3 suppression with vincristine, a chemotherapy agent used for aRMS treatment since the 1970s (42), would be more effective at inhibiting aRMS cell growth than either alone. To this end, we first performed an MTT assay using Rh28 cells expressing an empty vector or SFRP3 sh3 with vincristine (0-10 nM). While both SFRP3 inhibition and vincristine inhibited cell growth alone, the combination produced the greatest inhibition (Fig. 6A), as evidenced by the shRNA-drug dose curve shifting to the left.

While Rh28 cells appeared sensitized to vincristine in the presence of SFRP3 suppression *in vitro*, we next investigated the combination in our *in vivo* xenograft model of aRMS. Xenograft tumors were generated using Rh28 cells containing a doxycycline inducible SFRP3 shRNA (SFRP3 sh3) or empty vector as done previously. Once the tumors were palpable, mice were randomized to treatment with doxycycline plus weekly vincristine (or vehicle) injections. As expected, we found that vincristine alone or SFRP3 suppression alone inhibited tumor growth (Fig. 6B,C). However, the combination of vincristine and SFRP3 suppression was more effective than either treatment alone (Fig. 6D,E), and unexpectedly caused tumor regression. [To verify that doxycycline was not interfering with the chemotherapeutic property of vincristine, a shadow control group of mice were treated with vincristine plus the vehicle for doxycycline and compared to those being treated with vincristine. There was no difference between the groups, suggesting that indeed doxycycline was not interfering with vincristine (Supplementary Fig. 4).] In survival analysis, while

SFRP3 suppression alone and vincristine alone prolonged survival to an IACUC-approved endpoint, the combination was most effective (Fig. 6F).

At necropsy, the tumors arising from the SFRP3 suppression alone or vincristine alone treatment groups showed no notable changes in the histology when stained with H&E. However, both groups showed decreased cell proliferation as measured by Ki67, with the change caused by SFRP3 suppression being significant (Fig. 6G). Both also demonstrated a trend towards an increase in apoptosis, as measured by TUNEL staining (Fig. 6H). In the SFRP3 suppression plus vincristine group, five of seven mice had no detectable tumors. The remaining two mice had tiny remnant subcutaneous masses, the larger of which we embedded in paraffin and found on H&E to be composed mostly of fat cells. In summary, these data demonstrate the pre-clinical utility of SFRP3 suppression in combination with chemotherapy *in vivo*, suggesting that this approach should be explored further for its potential use in clinical care of patients with aRMS.

Discussion

This work demonstrates a novel role for the secreted Wnt inhibitor SFRP3 in supporting alveolar rhabdomyosarcoma (aRMS) tumorigenesis. SFRP3 is necessary for *in vitro* and *in vivo* aRMS cell growth. While SFRP3 levels were increased in PAX3-FOXO1-expressing cells (human myoblasts stably expressing PAX3-FOXO1 and human PAX3-FOXO1-positive aRMS cell lines), SFRP3 most likely cooperates with PAX3-FOXO1 to support aRMS tumorigenesis, rather than being a direct downstream target. Indeed neither SFRP3, nor any other SFRP family members, appear in a genome-wide screen identifying PAX3-FOXO1 binding sites (43). This cooperation is not unusual, as other genetic changes supporting aRMS tumorigenesis, including inactivation of $p16^{INK4a}$, work in concert with PAX3-FOXO1 rather than being transcriptional targets (28). Future work will elucidate the connection between PAX3-FOXO1 and SFRP3, which may also provide insight into the regulation of SFRP3.

In both our *in vitro* and *in vivo* studies, suppression of SFRP3 in aRMS cells blocked cell growth both by reducing proliferation and inducing apoptosis. These phenotypes are likely connected, as cell-cycle arrest can lead to secondary apoptosis if specific checkpoints are activated (44). In adult renal cancer SFRP3 supports cell survival, suggesting that it may also have a primary role in suppressing apoptosis (45). Future work examining the timing of the cell-cycle arrest and apoptosis in SFRP3-suppressed aRMS cells may reveal if they are related.

Previous studies have shown that SFRP3 can inhibit the differentiation-inducing effects of Wnt signaling on murine myoblasts, and that the addition of recombinant SFRP3 in regenerating murine skeletal muscle decreases nascent myotube formation, demonstrating that SFRP3 has a clear role in blocking differentiation (11). To this end we examined both myogenic differentiation and Wnt pathway status following SFRP3 suppression *in vitro* and *in vivo*. SFRP3 suppression induced myogenic differentiation as observed using a microarray approach and examination of markers of differentiation in tumors, but did not alter terminal differentiation (MF-20 staining) *in vitro*. In addition, while both shRNAs

promoted myogenic differentiation in the tumors, differences emerged as to which markers of differentiation were induced. Similarly, while we did not see evidence of Wnt pathway activation in the stable suppression system, the microarray analysis and levels of AXIN2 in the tumors did reflect this activation. While we do not fully understand the mechanisms causing these inconsistencies, most likely a combination of effects are responsible including differences in the microenvironment, differences between the shRNAs, and differences in the amplitude of SFRP3 suppression. Indeed, Wnt activation and repression has been shown to be finely tuned to SFRP levels (46). Future work will attempt to reconcile these differences.

Increased SFRP3 expression has been previously reported in metastatic renal carcinoma, required for cell growth and invasion (45). However, several other malignancies including prostate cancer, breast cancer, and fibrosarcoma demonstrate downregulation or inhibition of SFRPs (47, 48). While SFRPs were originally identified as Wnt signaling inhibitors, recently SFRPs such as SFRP1 have been shown to both potentiate and inhibit canonical Wnt signaling depending on a number of factors including SFRP concentration (mentioned above), cell type, and Frizzled receptor expression (46). This suggests that secreted Wnt inhibitors may have more complex signaling functions than previously thought, and that each SFRP will need to be investigated in a cell and cancer-specific context.

Most interesting for the pre-clinical aspects of this work were the combined SFRP3 genetic suppression plus vincristine xenograft experiments, which showed frank tumor regression. The mechanism of this treatment effect is not clear. One possibility is that SFRP3 suppression worked in combination with the microtubule-poisoning properties of vincristine (49) to kill the aRMS cells within the xenograft. However, since the combination *in vitro* was not as profound as that seen *in vivo*, other mechanisms may be at work, including the possibility that vincristine was exerting effects on the tumor microenvironment, including inhibiting angiogenesis (50). Regardless of mechanism, while genetic inhibition of SFRP3 in combination with vincristine is currently not feasible for treatment of human aRMS patients, a monoclonal antibody against another secreted frizzled related protein (SFRP2) has been developed, and is effective in a murine model of breast cancer (51). A similar monoclonal antibody against SFRP3 could be developed and tested for clinical efficacy.

The role of Wnt in RMS, like other developmental pathways Hedgehog, Hippo and Notch, is only beginning to be understood (15, 16, 26, 52). Unlike in most adult epithelial cancers, where Wnt/β-catenin activity is upregulated and oncogenic, in a $p53^{-/-}$/c-$fos^{-/-}$ mouse model of eRMS and in human eRMS cell lines, β-catenin activity is downregulated. Boosting β-catenin activity pharmacologically induces MyoD expression and promotes differentiation (13), and increasing Wnt signaling inhibits eRMS cell proliferation and induces differentiation (14). Three studies of human RMS tumor samples (including fusion-positive aRMS) showed low or absent nuclear β-catenin staining, with some cytoplasmic β-catenin staining (15, 53, 54). These data suggest that while β-catenin is present in RMS, Wnt pathway signaling is diminished. Importantly, this decrease is not due to inability to be activated, since treating the cells with Wnt3a ligand results in activation of the pathway (15). These cell biological findings will need to be reconciled with recent genomic data identifying activating β-catenin mutations in 3-7% of human eRMS samples, with 20% of

eRMS samples demonstrating nuclear (active) β-catenin staining (55). No β-catenin mutations were found in PAX3-FOXO1-positive aRMS samples, consistent with the observation that aRMS harbors fewer mutations than eRMS (55-57). Taken together, these data indicate a possibility for active β-catenin contributing to a subset of eRMS tumors, but show no evidence of a contribution to aRMS tumors.

In summary, we demonstrate that SFRP3 is upregulated in PAX3-FOXO1-positive human myoblasts and human aRMS cells. Genetic suppression of SFRP3 reduced aRMS growth *in vitro* and *in vivo*, suggesting that SFRP3 is required for aRMS tumorigenesis. aRMS cells in which SFRP3 has been suppressed are more sensitive to vincristine and this combination results in tumor regression in a xenograft model of aRMS. These data suggest that SFRPs and suppression of the Wnt pathway play an important role in aRMS, provide insight into the molecular mechanisms underlying aRMS, and may inform new strategies for aRMS treatment.

Supplementary Material

Refer to Web version on PubMed Central for supplementary material.

Acknowledgments

We thank the laboratories of Dr. Christopher Counter, Dr. David Kirsch, and Dr. Dan Wechsler (Duke University School of Medicine) for helpful discussions, and the laboratories of Dr. Oren Becher (Duke University School of Medicine) and Dr. Ben Alman (The Hospital for Sick Children, Toronto, Ontario, Canada and Duke University School of Medicine), for reagents and advice on β-catenin IHC. We thank the Duke Microarray Core facility (a Duke National Cancer Institute and a Duke Genomic and Computational Biology shared resource facility) for their technical support, microarray data management and feedback on the generation of the microarray data reported in this manuscript.

Financial support: This research was supported by NIH grants R01 CA122706 (C.M.L.), 5T32GM007184-35 (J.K.), T32 CA059365 (K.K.S., L.C.), and the V Foundation for Cancer Research, St. Baldrick's Foundation, Sarcoma Foundation of America, and A Collaborative Pediatric Cancer Research Award from Bear Necessities Pediatric Cancer Foundation and Rally Foundation (C.M.L.).

References

1. Huh WW, Skapek SX. Childhood rhabdomyosarcoma: new insight on biology and treatment. Curr Oncol Rep. 2010; 12:402–10. [PubMed: 20820958]
2. Saab R, Spunt SL, Skapek SX. Myogenesis and RhabdomyosarcomaThe Jekyll and Hyde of Skeletal Muscle. 2011; 94:197–234.
3. Hettmer S, Wagers AJ. Muscling in: Uncovering the origins of rhabdomyosarcoma. Nat Med. 2010; 16:171–3. [PubMed: 20134473]
4. Ognjanovic S, Linabery AM, Charbonneau B, Ross JA. Trends in childhood rhabdomyosarcoma incidence and survival in the United States, 1975-2005. Cancer. 2009; 115:4218–26. [PubMed: 19536876]
5. Skapek SX, Anderson J, Barr FG, Bridge JA, Gastier-Foster JM, Parham DM, et al. PAX-FOXO1 fusion status drives unfavorable outcome for children with rhabdomyosarcoma: a children's oncology group report. Pediatric blood & cancer. 2013; 60:1411–7. [PubMed: 23526739]
6. Galili N, Davis RJ, Fredericks WJ, Mukhopadhyay S, Rauscher FJ 3rd, Emanuel BS, et al. Fusion of a fork head domain gene to PAX3 in the solid tumour alveolar rhabdomyosarcoma. Nat Genet. 1993; 5:230–5. [PubMed: 8275086]
7. MacDonald BT, Tamai K, He X. Wnt/β-Catenin Signaling: Components, Mechanisms, and Diseases. Developmental Cell. 2009; 17:9–26. [PubMed: 19619488]

8. Clevers H. Wnt/β-Catenin Signaling in Development and Disease. Cell. 2006; 127:469–80. [PubMed: 17081971]

9. Bovolenta P, Esteve P, Ruiz JM, Cisneros E, Lopez-Rios J. Beyond Wnt inhibition: new functions of secreted Frizzled-related proteins in development and disease. Journal of Cell Science. 2008; 121:737–46. [PubMed: 18322270]

10. Jones SE, Jomary C. Secreted Frizzled-related proteins: searching for relationships and patterns. BioEssays. 2002; 24:811–20. [PubMed: 12210517]

11. Brack AS, Conboy IM, Conboy MJ, Shen J, Rando TA. A Temporal Switch from Notch to Wnt Signaling in Muscle Stem Cells Is Necessary for Normal Adult Myogenesis. Cell Stem Cell. 2008; 2:50–9. [PubMed: 18371421]

12. Polesskaya A, Seale P, Rudnicki MA. Wnt Signaling Induces the Myogenic Specification of Resident CD45+ Adult Stem Cells during Muscle Regeneration. Cell. 2003; 113:841–52. [PubMed: 12837243]

13. Singh S, Vinson C, Gurley CM, Nolen GT, Beggs ML, Nagarajan R, et al. Impaired Wnt Signaling in Embryonal Rhabdomyosarcoma Cells from p53/c-fos Double Mutant Mice. American Journal Of Pathology. 2010; 177:2055–66. [PubMed: 20829439]

14. Chen EY, Deran MT, Ignatius MS, Grandinetti KB, Clagg R, McCarthy KM, et al. Glycogen synthase kinase 3 inhibitors induce the canonical WNT/beta-catenin pathway to suppress growth and self-renewal in embryonal rhabdomyosarcoma. Proc Natl Acad Sci U S A. 2014; 111:5349–54. [PubMed: 24706870]

15. Annavarapu SR, Cialfi S, Dominici C, Kokai GK, Uccini S, Ceccarelli S, et al. Characterization of Wnt/beta-catenin signaling in rhabdomyosarcoma. Lab Invest. 2013; 93:1090–9. [PubMed: 23999248]

16. Crose LE, Galindo KA, Kephart JG, Chen C, Fitamant J, Bardeesy N, et al. Alveolar rhabdomyosarcoma-associated PAX3-FOXO1 promotes tumorigenesis via Hippo pathway suppression. J Clin Invest. 2013

17. McAllister RM, Melnyk J, Finkelstein JZ, Adams EC Jr, Gardner MB. Cultivation in vitro of cells derived from a human rhabdomyosarcoma. Cancer. 1969; 24:520–6. [PubMed: 4241949]

18. Hazelton BJ, Houghton JA, Parham DM, Douglass EC, Torrance PM, Holt H, et al. Characterization of cell lines derived from xenografts of childhood rhabdomyosarcoma. Cancer Res. 1987; 47:4501–7. [PubMed: 3607778]

19. Douglass EC, Valentine M, Etcubanas E, Parham D, Webber BL, Houghton PJ, et al. A specific chromosomal abnormality in rhabdomyosarcoma. Cytogenet Cell Genet. 1987; 45:148–55. [PubMed: 3691179]

20. Keleti J, Quezado MM, Abaza MM, Raffeld M, Tsokos M. The MDM2 oncoprotein is overexpressed in rhabdomyosarcoma cell lines and stabilizes wild-type p53 protein. Am J Pathol. 1996; 149:143–51. [PubMed: 8686737]

21. Whang-Peng J, Knutsen T, Theil K, Horowitz ME, Triche T. Cytogenetic studies in subgroups of rhabdomyosarcoma. Genes Chromosomes Cancer. 1992; 5:299–310. [PubMed: 1283318]

22. Khan J, Simon R, Bittner M, Chen Y, Leighton SB, Pohida T, et al. Gene expression profiling of alveolar rhabdomyosarcoma with cDNA microarrays. Cancer Res. 1998; 58:5009–13. [PubMed: 9823299]

23. Naini S, Etheridge KT, Adam SJ, Qualman SJ, Bentley RC, Counter CM, et al. Defining the Cooperative Genetic Changes That Temporally Drive Alveolar Rhabdomyosarcoma. Cancer Research. 2008; 68:9583–8. [PubMed: 19047133]

24. Borello U, Coletta M, Tajbakhsh S, Leyns L, De Robertis EM, Buckingham M, et al. Transplacental delivery of the Wnt antagonist Frzb1 inhibits development of caudal paraxial mesoderm and skeletal myogenesis in mouse embryos. Development. 1999; 126:4247–55. [PubMed: 10477293]

25. Barr FG, Nauta LE, Hollows JC. Structural analysis of PAX3 genomic rearrangements in alveolar rhabdomyosarcoma. Cancer Genet Cytogenet. 1998; 102:32–9. [PubMed: 9530337]

26. Belyea BC, Naini S, Bentley RC, Linardic CM. Inhibition of the Notch-Hey1 Axis Blocks Embryonal Rhabdomyosarcoma Tumorigenesis. Clin Cancer Res. 2011

27. Fang Y, Linardic CM, Richardson DA, Cai W, Behforouz M, Abraham RT. Characterization of the cytotoxic activities of novel analogues of the antitumor agent, lavendamycin. Mol Cancer Ther. 2003; 2:517–26. [PubMed: 12813130]
28. Linardic CM, Naini S, Herndon JE, Kesserwan C, Qualman SJ, Counter CM. The PAX3-FKHR Fusion Gene of Rhabdomyosarcoma Cooperates with Loss of p16INK4A to Promote Bypass of Cellular Senescence. Cancer Research. 2007; 67:6691–9. [PubMed: 17638879]
29. Kanazawa A, Tsukada S, Kamiyama M, Yanagimoto T, Nakajima M, Maeda S. Wnt5b partially inhibits canonical Wnt/beta-catenin signaling pathway and promotes adipogenesis in 3T3-L1 preadipocytes. Biochem Biophys Res Commun. 2005; 330:505–10. [PubMed: 15796911]
30. Westfall TA, Brimeyer R, Twedt J, Gladon J, Olberding A, Furutani-Seiki M, et al. Wnt-5/pipetail functions in vertebrate axis formation as a negative regulator of Wnt/beta-catenin activity. J Cell Biol. 2003; 162:889–98. [PubMed: 12952939]
31. Leyns L, Bouwmeester T, Kim SH, Piccolo S, De Robertis EM. Frzb-1 is a secreted antagonist of Wnt signaling expressed in the Spemann organizer. Cell. 1997; 88:747–56. [PubMed: 9118218]
32. Harper JW, Adami GR, Wei N, Keyomarsi K, Elledge SJ. The p21 Cdk-interacting protein Cip1 is a potent inhibitor of G1 cyclin-dependent kinases. Cell. 1993; 75:805–16. [PubMed: 8242751]
33. Jho EH, Zhang T, Domon C, Joo CK, Freund JN, Costantini F. Wnt/beta-catenin/Tcf signaling induces the transcription of Axin2, a negative regulator of the signaling pathway. Mol Cell Biol. 2002; 22:1172–83. [PubMed: 11809808]
34. Yan D, Wiesmann M, Rohan M, Chan V, Jefferson AB, Guo L, et al. Elevated expression of axin2 and hnkd mRNA provides evidence that Wnt/beta -catenin signaling is activated in human colon tumors. Proc Natl Acad Sci U S A. 2001; 98:14973–8. [PubMed: 11752446]
35. Lustig B, Jerchow B, Sachs M, Weiler S, Pietsch T, Karsten U, et al. Negative feedback loop of Wnt signaling through upregulation of conductin/axin2 in colorectal and liver tumors. Mol Cell Biol. 2002; 22:1184–93. [PubMed: 11809809]
36. Tang X, Lucas JE, Chen JL, LaMonte G, Wu J, Wang MC, et al. Functional interaction between responses to lactic acidosis and hypoxia regulates genomic transcriptional outputs. Cancer Res. 2012; 72:491–502. [PubMed: 22135092]
37. Valenta T, Lukas J, Korinek V. HMG box transcription factor TCF-4's interaction with CtBP1 controls the expression of the Wnt target Axin2/Conductin in human embryonic kidney cells. Nucleic Acids Res. 2003; 31:2369–80. [PubMed: 12711682]
38. Ishiguro H, Shimokawa T, Tsunoda T, Tanaka T, Fujii Y, Nakamura Y, et al. Isolation of HELAD1, a novel human helicase gene up-regulated in colorectal carcinomas. Oncogene. 2002; 21:6387–94. [PubMed: 12214280]
39. Ashihara E, Takada T, Maekawa T. Targeting the canonical Wnt/beta-catenin pathway in hematological malignancies. Cancer Sci. 2015
40. Wu ZQ, Li XY, Hu CY, Ford M, Kleer CG, Weiss SJ. Canonical Wnt signaling regulates Slug activity and links epithelial-mesenchymal transition with epigenetic Breast Cancer 1, Early Onset (BRCA1) repression. Proc Natl Acad Sci U S A. 2012; 109:16654–9. [PubMed: 23011797]
41. Hitchins L, Fletcher F, Allen S, Dhoot GK. Role of Sulf1A in Wnt1- and Wnt6-induced growth regulation and myoblast hyper-elongation. FEBS Open Bio. 2013; 3:30–4.
42. Crist W, Gehan EA, Ragab AH, Dickman PS, Donaldson SS, Fryer C, et al. The Third Intergroup Rhabdomyosarcoma Study. J Clin Oncol. 1995; 13:610–30. [PubMed: 7884423]
43. Cao L, Yu Y, Bilke S, Walker RL, Mayeenuddin LH, Azorsa DO, et al. Genome-Wide Identification of PAX3-FKHR Binding Sites in Rhabdomyosarcoma Reveals Candidate Target Genes Important for Development and Cancer. Cancer Research. 2010; 70:6497–508. [PubMed: 20663909]
44. Orth JD, Loewer A, Lahav G, Mitchison TJ. Prolonged mitotic arrest triggers partial activation of apoptosis, resulting in DNA damage and p53 induction. Mol Biol Cell. 2012; 23:567–76. [PubMed: 22171325]
45. Hirata H, Hinoda Y, Ueno K, Majid S, Saini S, Dahiya R. Role of Secreted Frizzled-Related Protein 3 in Human Renal Cell Carcinoma. Cancer Research. 2010; 70:1896–905. [PubMed: 20160027]

46. Xavier CP, Melikova M, Chuman Y, Uren A, Baljinnyam B, Rubin JS. Secreted Frizzled-related protein potentiation versus inhibition of Wnt3a/beta-catenin signaling. Cell Signal. 2014; 26:94–101. [PubMed: 24080158]
47. Surana R, Sikka S, Cai W, Shin EM, Warrier SR, Tan HJ, et al. Secreted frizzled related proteins: Implications in cancers. Biochim Biophys Acta. 2013; 1845:53–65. [PubMed: 24316024]
48. Guo Y, Xie J, Rubin E, Tang YX, Lin F, Zi X, et al. Frzb, a Secreted Wnt Antagonist, Decreases Growth and Invasiveness of Fibrosarcoma Cells Associated with Inhibition of Met Signaling. Cancer Research. 2008; 68:3350–60. [PubMed: 18451162]
49. Himes RH, Kersey RN, Heller-Bettinger I, Samson FE. Action of the vinca alkaloids vincristine, vinblastine, and desacetyl vinblastine amide on microtubules in vitro. Cancer Res. 1976; 36:3798–802. [PubMed: 954003]
50. Mabeta P, Pepper MS. A comparative study on the anti-angiogenic effects of DNA-damaging and cytoskeletal-disrupting agents. Angiogenesis. 2009; 12:81–90. [PubMed: 19214765]
51. Fontenot E, Rossi E, Mumper R, Snyder S, Siamakpour-Reihani S, Ma P, et al. A novel monoclonal antibody to secreted frizzled-related protein 2 inhibits tumor growth. Mol Cancer Ther. 2013; 12:685–95. [PubMed: 23604067]
52. Tostar U, Toftgard R, Zaphiropoulos PG, Shimokawa T. Reduction of human embryonal rhabdomyosarcoma tumor growth by inhibition of the hedgehog signaling pathway. Genes & cancer. 2010; 1:941–51. [PubMed: 21779473]
53. Ng TL, Gown AM, Barry TS, Cheang MC, Chan AK, Turbin DA, et al. Nuclear beta-catenin in mesenchymal tumors. Mod Pathol. 2005; 18:68–74. [PubMed: 15375433]
54. Bouron-Dal Soglio D, Rougemont AL, Absi R, Giroux LM, Sanchez R, Barrette S, et al. Beta-catenin mutation does not seem to have an effect on the tumorigenesis of pediatric rhabdomyosarcomas. Pediatr Dev Pathol. 2009; 12:371–3. [PubMed: 19222307]
55. Chen X, Stewart E, Shelat AA, Qu C, Bahrami A, Hatley M, et al. Targeting oxidative stress in embryonal rhabdomyosarcoma. Cancer Cell. 2013; 24:710–24. [PubMed: 24332040]
56. Shern JF, Chen L, Chmielecki J, Wei JS, Patidar R, Rosenberg M, et al. Comprehensive genomic analysis of rhabdomyosarcoma reveals a landscape of alterations affecting a common genetic axis in fusion-positive and fusion-negative tumors. Cancer Discov. 2014; 4:216–31. [PubMed: 24436047]
57. Shukla N, Ameur N, Yilmaz I, Nafa K, Lau CY, Marchetti A, et al. Oncogene mutation profiling of pediatric solid tumors reveals significant subsets of embryonal rhabdomyosarcoma and neuroblastoma with mutated genes in growth signaling pathways. Clin Cancer Res. 2012; 18:748–57. [PubMed: 22142829]

Statement of Translational Relevance

Rhabdomyosarcoma (RMS) is the most common soft-tissue sarcoma of childhood and adolescence. While embryonal RMS (eRMS) has seen improved outcomes in the last 30 years, other RMS histologic groups including fusion-positive alveolar RMS (aRMS) continue to have lower survival rates. Since PAX3-FOXO1, a signature gene fusion product driving aRMS, has not yet been targeted pharmacologically, it is critical to identify cellular signaling pathways downstream of or cooperating with PAX3-FOXO1 that mediate its tumorigenic properties. Understanding how these pathways support aRMS initiation and maintenance will help to identify therapeutic targets. Here, we demonstrate that the secreted Wnt inhibitor SFRP3 is one such protein mediating PAX3-FOXO1-associated tumorigenesis. Suppression of SFRP3 in vitro and in vivo inhibits growth of PAX3-FOXO1-positive aRMS cells and tumors, respectively. SFRP3 inhibition also sensitizes aRMS cells to vincristine, a chemotherapeutic backbone of RMS therapy, suggesting that targeting SFRP3 may be a potential strategy for treating aRMS.

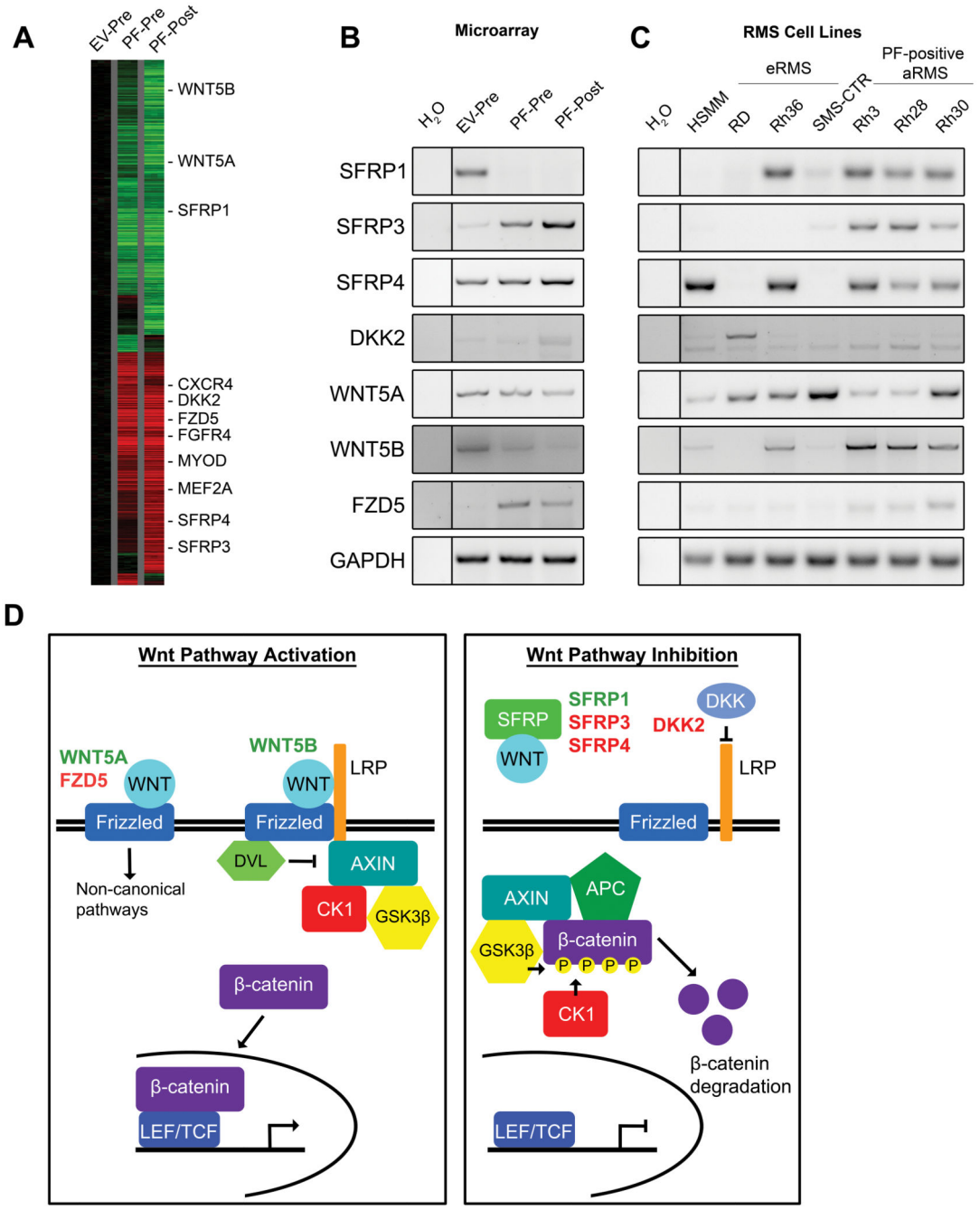

Figure 1. Secreted Wnt inhibitors, including SFRP3, are upregulated in PAX3-FOXO1-expressing primary human myoblasts and in human aRMS cell lines

(A) Wnt pathway genes identified through transcriptome profiling to be differentially regulated in the PF pre-senescence bypass (PF-Pre) or PF post-senescence bypass (PF-Post) groups when compared to the empty vector pre-senescence (EV-Pre) group. *CXCR4*, *MYOD*, *MEF2A*, and *FGFR4* are known to be upregulated in response to PAX3-FOXO1 and served as internal controls. Portions of these expression data were previously reported (16) and this image is modified with permission from the *Journal of Clinical Investigation*.

Expression patterns of Wnt pathway genes identified in the array were **(B)** verified through RT-PCR and **(C)** assayed in HSMM, eRMS, and aRMS cells using RT-PCR. SFRP3 was chosen for further analysis due to its expression pattern. **(D)** Diagram of the canonical Wnt pathway. Wnt pathway genes identified in the microarray from (A) are labeled in green (downregulated) or red (upregulated). WNT5B is both a canonical and non-canonical Wnt.

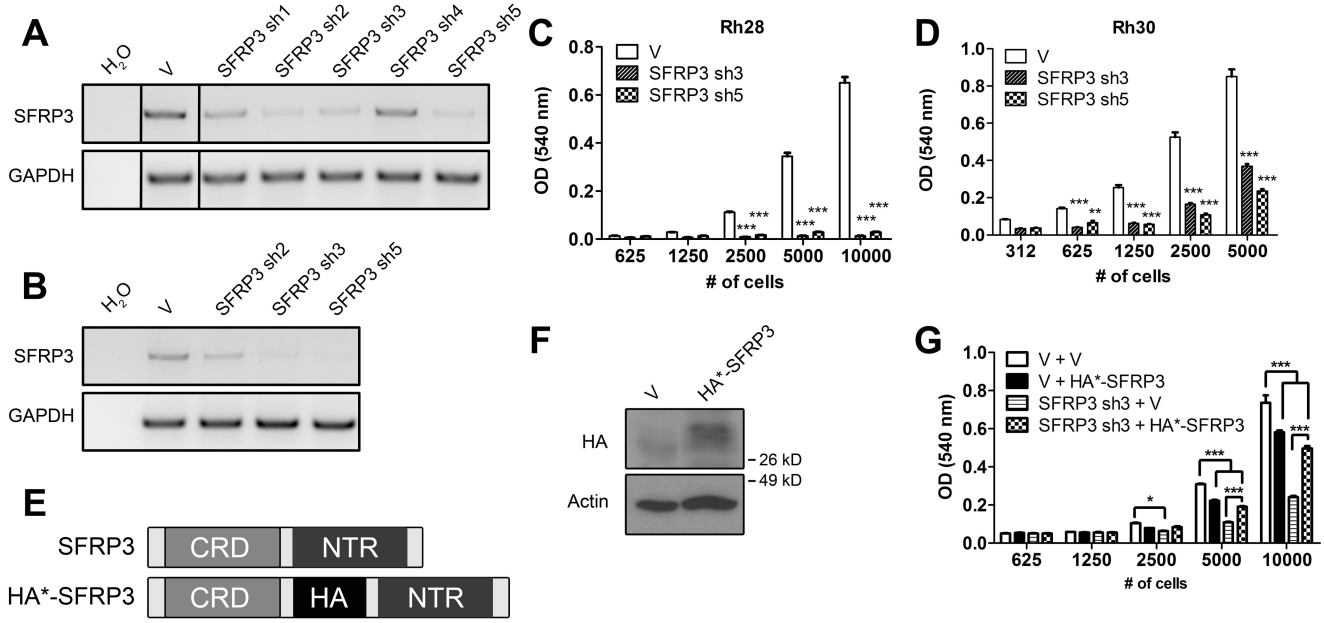

Figure 2. SFRP3 suppression inhibits aRMS cell growth

shRNAs against SFRP3 were stably expressed in aRMS cell lines Rh28 **(A)** and Rh30 **(B)** using a lentiviral vector. SFRP3 sh3 and sh5 consistently showed robust suppression of SFRP3 as measured by RT-PCR; therefore, were chosen for further study. Both SFRP3 sh3 and sh5 reduced cell growth of Rh28 **(C)** and Rh30 **(D)** cells as measured by a standard MTT assay. **(E)** To confirm that the decrease in cell growth is not due to shRNA off-target effects, a murine SFRP3 containing an HA tag (HA*-SFRP3) was used as a rescue construct. (**F)** HA*-SFRP3 was stably expressed in Rh28 cells and detected by immunoblot. **(G)** HA*-SFRP3, when co-expressed with a doxycycline-inducible version of SFRP3 sh3, partially rescued the SFRP3 sh3-mediated decreased cell growth. *p<0.05, **p<0.01, ***p<0.001

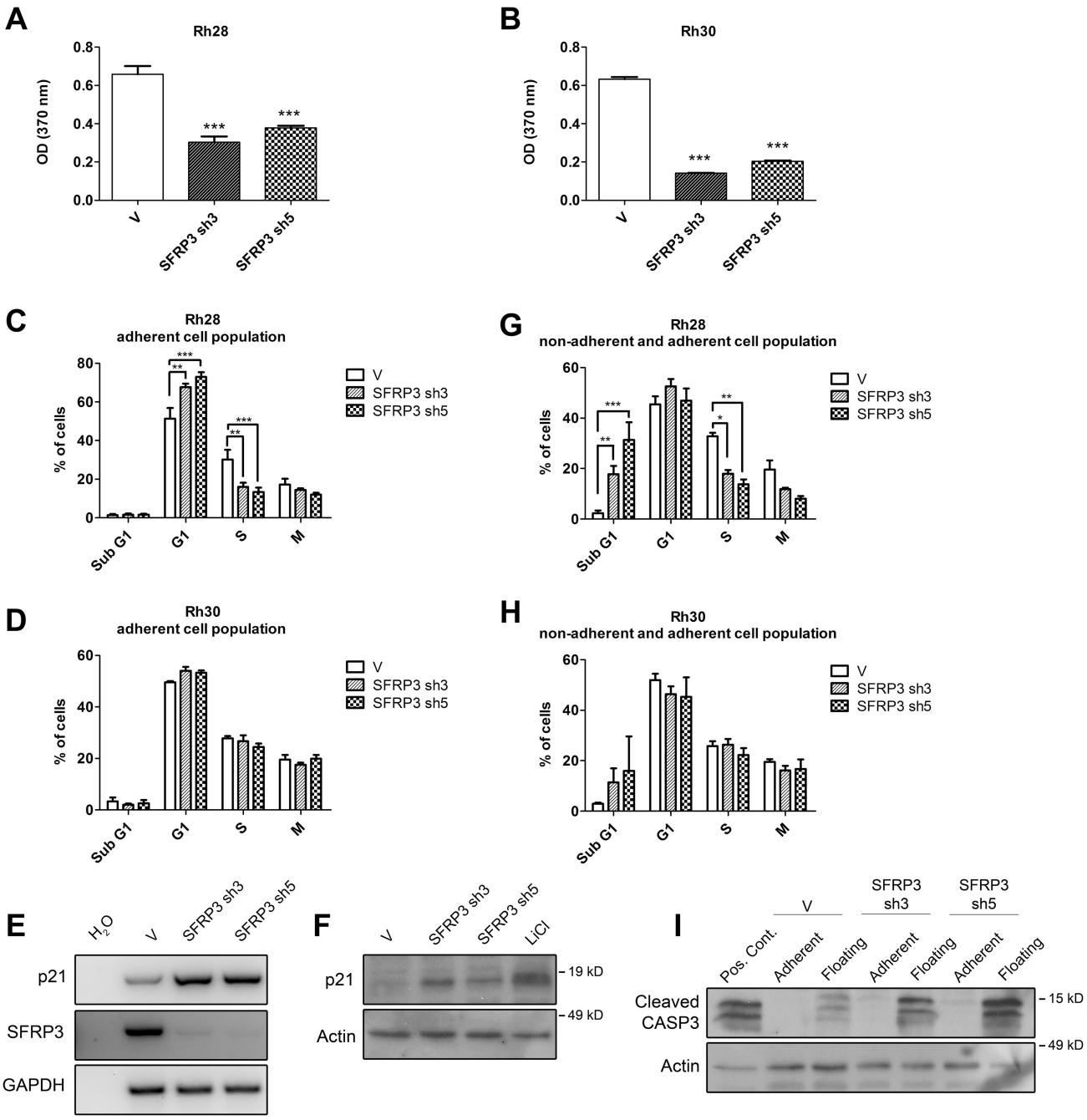

Figure 3. SFRP3 suppression inhibits cell proliferation, causes a G_1 arrest, and increases apoptosis

SFRP3 suppression inhibits cell proliferation of Rh28 **(A)** and Rh30 **(B)** cells as measured by BrdU incorporation. SFRP3 suppression causes a G_1 arrest in Rh28 **(C)** and Rh30 **(D)** cells as measured by cell cycle analysis using PI staining and flow cytometry, although statistically significant only in Rh28 cells. Cell cycle data shown are the averages of three (Rh28) or four (Rh30) independent experiments. Consistent with a G_1 arrest, SFRP3 suppression elevates p21 levels in Rh28 cells as measured by RT-PCR **(E)** and immunoblot

(F). LiCl served as a positive control. While no evidence of apoptosis was observed in the adherent cell population assayed in (A) through (F), when non-adherent cells were included in the analysis, apoptosis in response to SFRP3 suppression was detected in Rh28 **(G)** and Rh30 **(H)** cells. Data shown are the averages of three (Rh28) or five (Rh30) independent experiments. **(I)** Apoptosis in response to SFRP3 suppression was confirmed in Rh28 cells using immunoblots for cleaved caspase-3. *p<0.05, **p<0.01, ***p<0.001

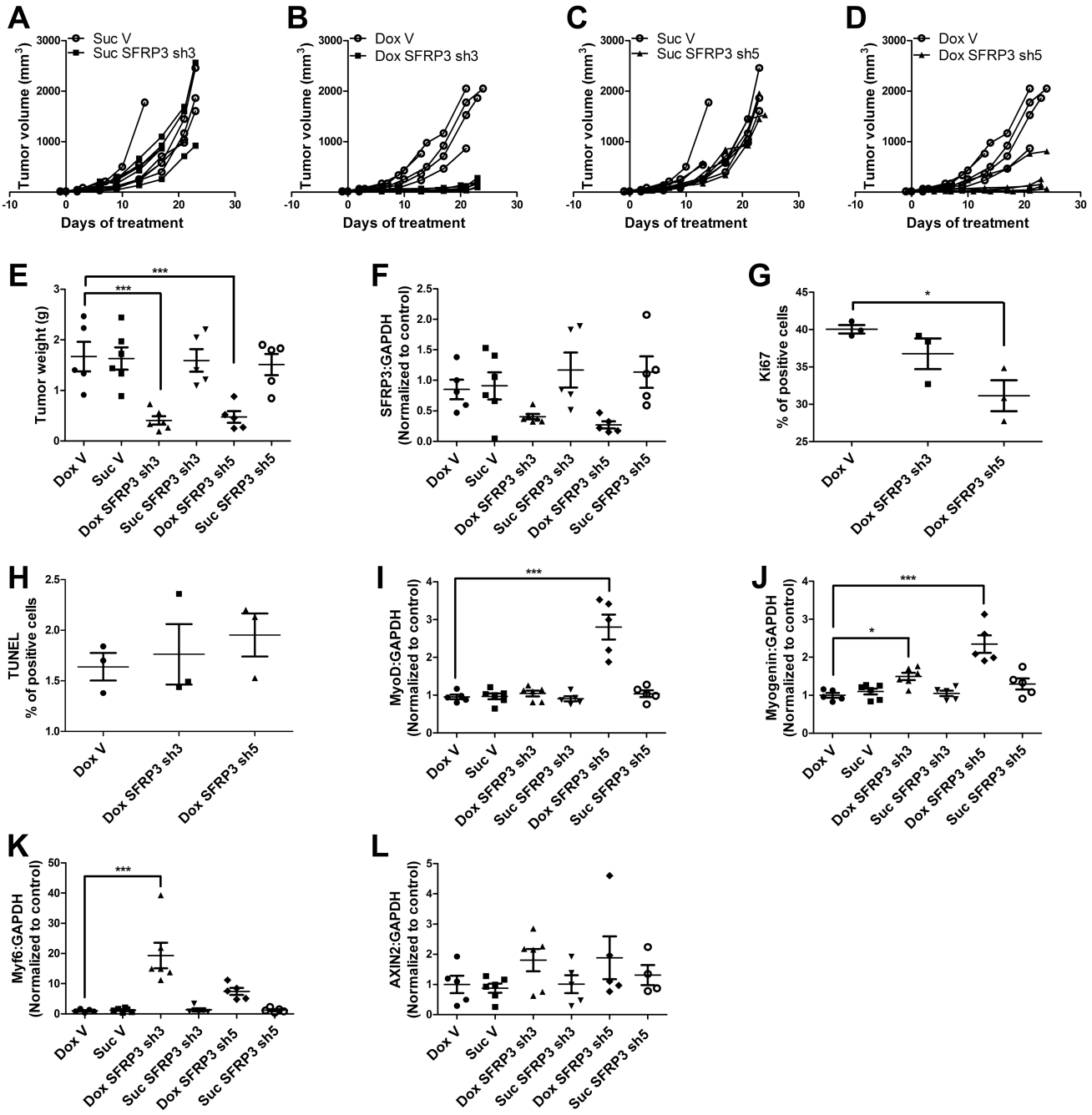

Figure 4. SFRP3 suppression inhibits tumor growth *in vivo*

Rh28 cells expressing doxycycline-inducible shRNAs against SFRP3 (or vector) were injected subcutaneously into the flanks of SCID/*beige* mice. Once tumors were palpable, mice were randomly assigned to doxycycline or sucrose (control) group. Tumor dimensions were measured twice a week using calipers. In mice treated with sucrose, SFRP3 sh3 **(A)** and sh5 **(C)** showed no reduction in growth. In the doxycycline treated groups, SFRP3 suppression due to sh3 **(B)** or sh5 **(D)** reduced tumor growth. **(E)** Following 23 days of exposure to doxycycline or sucrose or when an IACUC-defined endpoint was reached, mice

were sacrificed and tumors were excised and weighed. SFRP3 suppression reduced tumor weight. **(F)** SFRP3 levels within the tumors were measured by RT-PCR to confirm knockdown. Tumors were fixed, embedded in paraffin, sectioned, and analyzed using IHC for cell proliferation (Ki67) and apoptosis (TUNEL). **(G)** SFRP3 sh5 significantly reduced, while SFRP3 sh3 showed a trend towards reducing, cell proliferation. **(H)** Both SFRP3 sh3 and sh5 show a trend towards increasing apoptosis, although not statistically significant. SFRP3 shRNAs also elevated levels of markers of muscle differentiation, *MYOD1* **(I)**, *MYOG* **(J)**, and *MYF6* (also known as *MRF4)* **(K)**, as measured by qPCR. **(L)** SFRP3 shRNAs also modestly, though non-significantly, increased levels of *AXIN2*, a transcriptional target of β-catenin, as measured by qPCR. *$p<0.05$, ***$p<0.001$ when compared to Dox V.

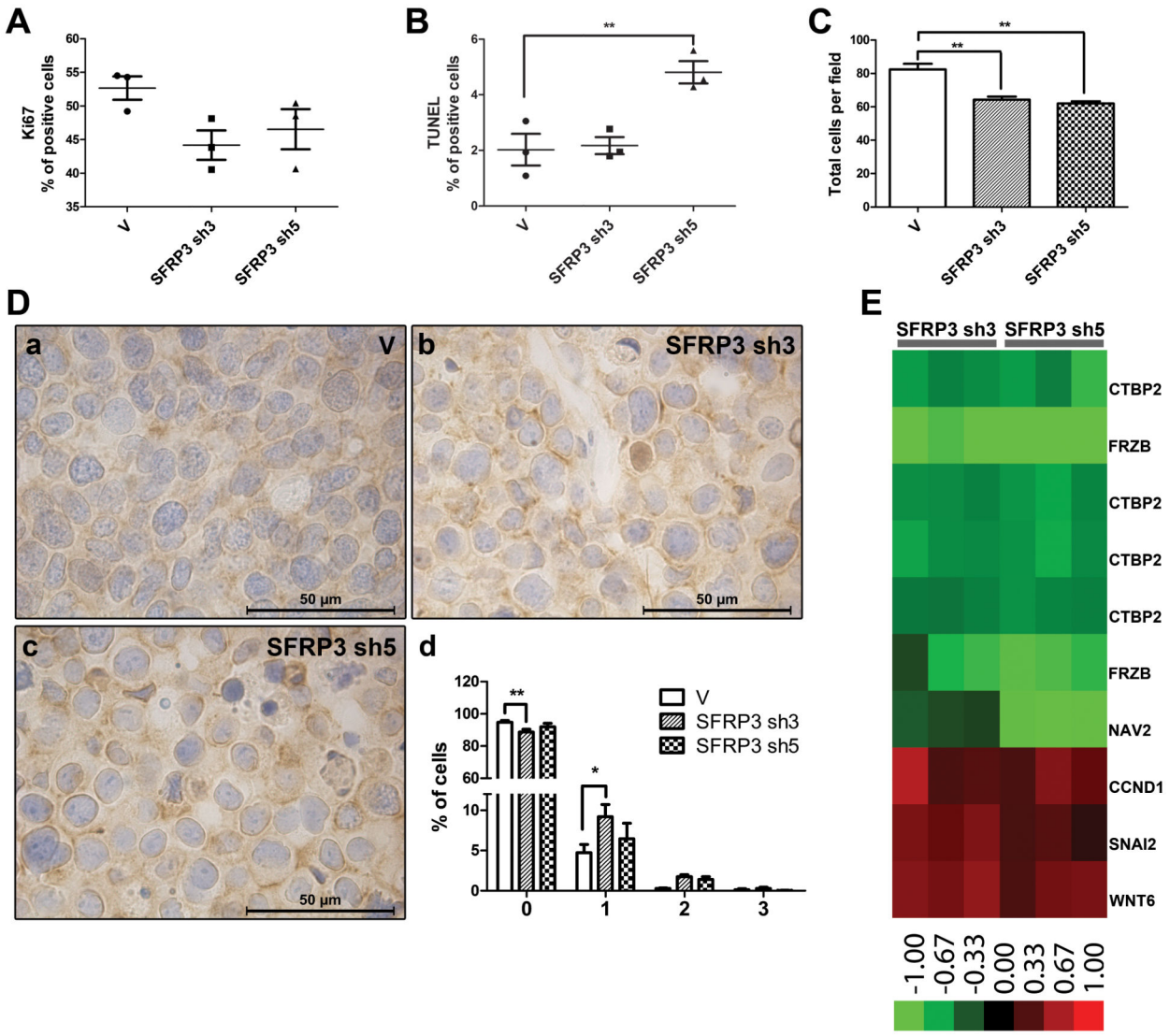

Figure 5. SFRP3 suppression increases β-catenin expression

Tumors were generated and harvested as described in Fig. 4, except that they were harvested after only 14 days to capture early events. Tumors were fixed, embedded in paraffin, sectioned, and analyzed using IHC for cell proliferation (Ki67), apoptosis (TUNEL), and β-catenin. SFRP3 suppression shows a trend towards reduced proliferation **(A)** and increased apoptosis, significant for SFRP3 sh5 **(B)**. SFRP3 suppression reduced the number of cells per field **(C)** and **(D, a-c)**, but increased nuclear β-catenin staining **(D, a-d)**, suggesting increased Wnt signaling activity. Representative sections shown in **(D, a-c). (E)** Heatmap of the expression changes of the indicated Wnt-related genes consistently altered by SFRP3 suppression. The filter criteria required at least 4 observations with an abs value of >= 0.3. The color bar has a value of 1. *p<0.05, **p<0.01

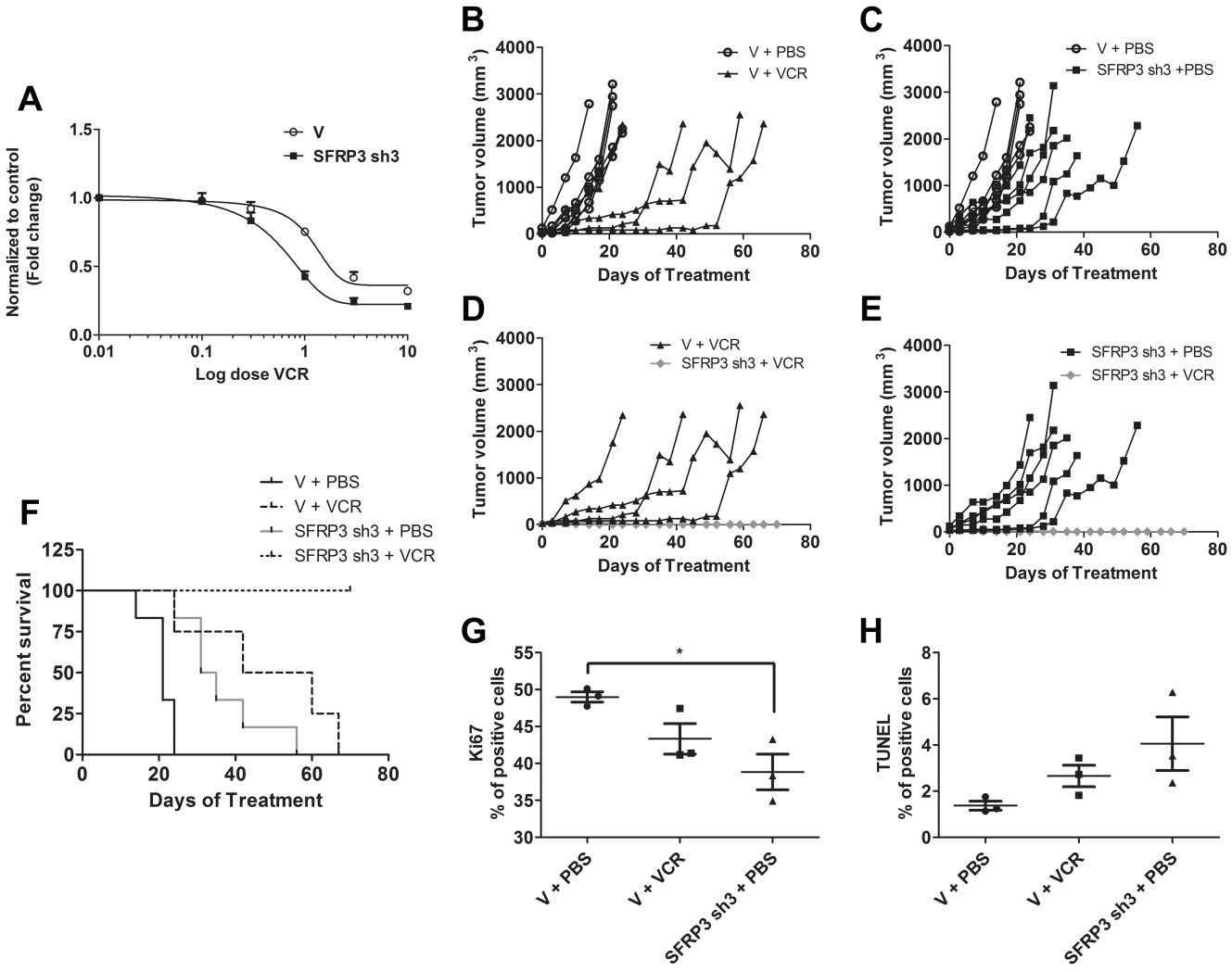

Figure 6. SFRP3 suppression in combination with vincristine inhibits aRMS cell and tumor growth and causes tumor regression

(A) Rh28 cells stably expressing a doxycycline-inducible shRNA against SFRP3 (SFRP3 sh3) or empty vector (V) were treated with 2ug/mL doxycycline and increasing doses of vincristine. As measured by MTT assay, the combination of SFRP3 suppression and vincristine was more effective than vincristine alone at inhibiting cell growth. Rh28 xenograft tumors were generated containing an empty vector (V) or a doxycycline-inducible SFRP3 shRNA (SFRP3 sh3). All mice received doxycycline and either vincristine (VCR) or PBS. Both vincristine (V+PBS) **(B)** and SFRP3 suppression (SFRP3 sh3+PBS) **(C)** decreased tumor growth as compared to empty vector (V+PBS). The combination of vincristine and SFRP3 suppression (SFRP3 sh3+VCR) was most effective at decreasing tumor growth, inhibiting more than vincristine (V+VCR) **(D)** or SFRP3 suppression (SFRP3 sh3+PBS) **(E)** alone. **(F)** While both SFRP3 suppression (SFRP3 sh3+PBS) and vincristine (V+VCR) increased survival compared to control (V+PBS), the combination of SFRP3 suppression and vincristine (SFRP3 sh3+VCR) prolonged survival the longest. **(G)** SFRP3

suppression significantly decreased cell proliferation when compared to empty vector. **(H)** Both SFRP3 suppression and vincristine show a trend towards an increase in apoptosis.